13

Molecular Design of Novel Self-Oscillating Polymer Chains Fuelled by Organic Acid Under Constant Condition

Yusuke Hara
Nanosystem Research Institute (NRI),
National Institute of Advanced Industrial Science and Technology (AIST)
Japan

1. Introduction

Stimuli-responsive polymers system, which responds to external stimuli such as temperature, pH, electric fields, etc., have been much investigated in order to apply to actuators, artificial muscle, drug delivery systems (DDS), shape-memory, molecular recognition material, separation-system and purification material, etc. [1-21] However, the conventional-type stimuli-responsive polymer system provides only one unique action to the external stimulus. On the other hand, many biological systems, such as the brain waves, autonomic heartbeat and periodic hormone secretion, show autonomous oscillations and respond to external stimuli. If we construct the autonomous polymer system like a living organism with tailor-made design, unprecedented polymer system would be realized. In this study, in order to construct the autonomous polymer system like a living organism, the Belousov-Zhabotinsky (BZ) has been utilized as the chemical energy source of the autonomous motion for polymer systems.

The BZ reaction is well known as an oscillating reaction accompanying spontaneous redox oscillations to generate a wide variety of nonlinear phenomena, e.g., target or spiral pattern in an unstirred solution, and periodicity, multi-periodicity, or chaos in a stirred solution [22-30]. The overall process of the BZ reaction is the oxidization of an organic substrate by an oxidizing agent in the presence of the catalyst under strong acidic conditions. In the BZ reaction, the metal catalyst undergoes spontaneous redox oscillation. In the case of utilizing the ruthenium tris(2,2′-bipyridine) that is the metal catalyst of the BZ reaction, the Ru catalyst has the different solubility in the reduced and oxidized states, respectively: the reduced Ru catalyst has a hydrophobic property, and the oxidized one has a hydrophilic one. In order to cause the self-oscillation of the polymer system (liner-polymer chain and polymer gel), polymer main-chain covalently bonded to the (ruthenium (4-vinyl-4′-methyl-2,2-bipyridine) bis(2,2′-bipyridine)bis(hexafluorophosphate)) ($Ru(bpy)_3$) as a catalyst of the BZ reaction were synthesized [31-33]. The main-chain of the self-oscillating polymer system adopted thermoresponsive poly(Nisopropylacrylamide) (poly(NIPAAm)). As a result, the polymer system cause the autonomous and spontaneous aggregation-disaggregation self-oscillation for the linear-polymer chain and the swelling-deswelling self-oscillation for the polymer gel under the constant temperature conditions with the coexistence of the BZ substrates other than the metal catalyst. However, operating condition of the self-oscillating

polymer system was limited to non-biological environment where the strong acid and the oxidant coexist. In order to expand the application field of the self-oscillating polymer system, I proposed more sophisticated molecular design to cause the self-oscillation under the biological condition. This polymer system incroporates the BZ substrates other than organic substrate into the conventional-type self-oscillating polymer chain (poly(NIPAAm-*co*-Ru(bpy)$_3$). As the first step for this purpose, acrylamide-2-methylpropane sulfonic acid (AMPS) was incorporated into the poly(NIPAAm-*co*-Ru(bpy)$_3$) chain as a pH and a solubility control site [34-37]. Moreover, as the second step, methacryl-amido-propyltrimethylammonium chloride (MAPTAC) with a positively charged group was incorporated into the conventional-type self-oscillating polymer chain as a capture site for an anionic oxidizing agent (bromate ion) [38]. The bromate ion was introduced into the polymer chain through the ion-exchange process. Finally, both the pH-control and the oxidant supply sites were incorporated into the polymer chain at same time. As a result, the aggregation-disaggregaiton self-oscillation of the novel polymer chain under the biological condition was observed [39].

2. Experimental section

2.1 Polymerization

2.1.1 Synthesis of poly(NIPAAm-*co*-Ru(bpy)$_3$-*co*-AMPS)

Using N-isopropylacrylamide (NIPAAm), AMPS, Ru(bpy)$_3$ monomer (ruthenium (4-vinyl-4′-methyl-2,2-bipyridine)bis(2,2′-bipyridine)bis(hexafluorophosphate)) and 2,2′-azobisisobutyronitrile (AIBN) as an initiator, poly(NIPAAm-*co*-Ru(bpy)$_3$ -*co*-AMPS) (Figure 1) was synthesized by radical polymerization in a mixture of methanol and water (1:1 wt/wt%) under a total monomer concentration of 20 wt%. The feed composition (wt%) was as follows; NIPAAm : Ru(bpy)$_3$: AMPS = 40 :10 : 50. The polymerization was carried out at 60 °C for 24 h in vacuo. The resulting reaction mixture was dialyzed against water for 10 days followed by methanol for 3 days, and then freeze-dried.

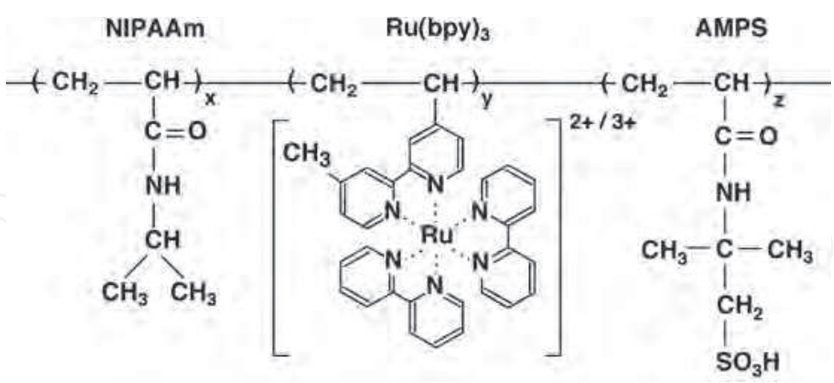

Fig. 1. The chemical structure of poly(NIPAAm-*co*-Ru(bpy)$_3$-*co*-AMPS).

2.1.2 Synthesis of poly(NIPAAm-*co*-Ru(bpy)$_3$-*co*-MAPTAC) with BrO_3^- as the counter ion

Using NIPAAm (2.5 g), MAPTAC (6.5 g), Ru(bpy)$_3$ monomer (1.0 g), and AIBN (0.35 g) as an initiator, poly(NIPAAm-*co*-Ru(bpy)$_3$-*co*-MAPTAC) was synthesized by radical polymerization in methanol (40 g). The polymerization was carried out at 60 °C for 24 h in vacuo. The resulting reaction mixture was dialyzed against methanol for 3 days and then

water for 4 days. For exchanging the counter ion, the polymer was dissolved in $NaBrO_3$ aqueous solution (1 M) and dialyzed against pure water for 30 days with repeating exchanging the water to remove excess Na^+ and BrO_3^- ions, and then freeze-dried.

2.1.3 Synthesis of poly(NIPAAm-*co*-Ru(bpy)$_3$) and poly(NIPAAm-*co*-Ru(bpy)$_3$-*co*-MAPTAC) without BrO_3^- as the counter ion

Poly(NIPAAm-*co*-Ru(bpy)$_3$) was synthesized by radical polymerization in a methanol (31 g) under a total monomer concentration of 20 wt %, using NIPAAm (9.0g) and Ru(bpy)$_3$ (1.0 g) and AIBN (0.35 g) as an initiator. Utilizing NIPAAm (8.15 g), MAPTAC (0.85 g), Ru(bpy)$_3$ (1.0 g) and AIBN (0.35 g), poly(NIPAAm-*co*-Ru(bpy)$_3$-*co*-MAPTAC) was synthesized in a methanol (31 g) under the total concentration of 20 wt %. These polymerizations were carried out at 60°C for 24 h *in vacuo*. These resulting reaction mixtures were dialyzed against graded series of water/methanol mixtures, for 1day each in 0, 25, 50, 75, and 100 wt % of water, and then freeze-dried.

2.1.4 Synthesis of poly(NIPAAm-co-Ru(bpy)$_3$-co-AMPS-co-MAPTAC) with BrO_3^-, Br^- and H^+ as the counter ions.

The poly(NIPAAm-*co*-Ru(bpy)$_3$-*co*-AMPS-*co*-MAPTAC) (Figure 10) was synthesized by radical polymerization. NIPAAm (1.20g), Ru(bpy)$_3$ monomer (1.28 g), AMPS (13.05g), MAPTAC (0.47g) and 2,2′-azobis(2-methylbutyronitrile)isobutyronitrile (V-59) (0.41 g) as an initiator were dissolved in the mixture of methanol (31.80g) and water (31.80g) which was degassed and nitrogen-saturated under a total monomer concentration of 20 wt%. The polymerization was carried out at 80℃ for 24 h in vacuo. The resulting reaction mixture was dialyzed against methanol for 3 days and then water for 4 days. For exchanging counter ions, the polymer was dissolved in NaBrO3 (1M) and NaBr (0.5M) aqueous solution and dialyzed against pure water for 30 days with repeating exchanging the water to remove excess Na^+, Br^- and BrO_3^- ions. The counter ion in the AMPS site is changed to Na^+ through this counter ion exchange process. Therefore, in the next step, the counter ion in the AMPS site was exchanged to H^+ using ion-exchange resin, and then freeze-dried. To prevent bromine formation, the polymer solution was frozen immediately after collecting it. It should be noticed that the freeze-dried polymer chain with the oxidizing agent as the counter ion has explosive properties.

2.2 Measurement

2.2.1 Measurement of lower critical solution temperature (LCST)

The lower critical solution temperature (LCST) of the polymer solution was measured under reduced and oxidized states, by using $Ce(SO_4)_2$ as an oxidizing agent and $Ce_2(SO_4)_3$ as a reducing agent, respectively. The polymer solutions (0.5wt%) of poly(NIPAAm-*co*-Ru(bpy)$_3$) and poly(NIPAAm-*co*-Ru(bpy)$_3$-*co*-MAPTAC) were prepared by dissolving the polymer in a 0.3M HNO_3 aqueous solution and adding 1.0 mM $Ce(SO_4)_2$ or 1.0 mM $Ce_2(SO_4)_3$, respectively. The LCST measurements were carried out with a spectrophotometer (Shimazu, Model UV-2500) equipped with magnetic stirrers and a thermostatic controller. In this measurement, the 570 nm wavelength was used because it is the isosbestic point for the reduced and oxidized states of Ru(bpy)$_3$. The transmittance (%) of the polymer solution at 570 nm was then recorded by raising the temperature at a rate of 0.5 °C/min.

2.2.2 Measurement of self-oscillations for poly(NIPAAm-*co*-Ru(bpy)$_3$-*co*-AMPS) solution under acid-free condition

The AMPS-containing polymer solutions were prepared by dissolving the polymer (2.5 wt%) into an aqueous solution containing the two BZ substrates (malonic acid (MA) and sodium bromate ($NaBrO_3$)). The transmittance self-oscillations for the polymer solutions were measured under constant temperature and stirring. In order to detect the transmittance change which is based on the autonomous aggregation-disaggregation change, 570-nm wavelength was used because it is the isosbestic point for the reduced and oxidized states of the Ru(bpy)$_3$. The time course of the transmittance at 570 nm was monitored by a spectrophotometer.

2.2.3 Measurement of self-oscillations for poly(NIPAAm-*co*-Ru(bpy)$_3$-*co*-MAPTAC) solution under oxidant-free condition

Polymer solutions were prepared by dissolving the MAPTAC-containing polymer (5.0 wt%) into an aqueous solution containing the two BZ substrates (0.1 M malonic acid and 0.3 M sulfuric acid). The optical transmittance oscillations for the polymer solutions were measured under constant temperature and stirring. The time course of transmittance at 570nm was monitored by a spectrophotometer.

2.2.4 Measurement of self-oscillations for poly(NIPAAm-*co*-Ru(bpy)$_3$) and poly(NIPAAm-*co*-Ru(bpy)$_3$-*co*-MAPTAC) without the BrO_3^- as the counter ion in the presence of the three BZ substrates other than the metal catalyst

The transmittance self-oscillation was measured by utilizing the poly(NIPAAm-*co*-Ru(bpy)$_3$) (polymer concentration: 0.25 wt %) and poly(NIPAAm-*co*-Ru(bpy)$_3$-*co*-MAPTAC) (polymer concentrations: 0.25, 0.75 and 1.00 wt %) solutions, which were prepared by dissolving the polymer into an aqueous solution containing the three BZ substrates (0.1 M malonic acid, 0.25 M sodium bromate and 0.3M nitric acid). The transmittance self-oscillations of the polymer solutions were measured at the constant temperature (20°C) while stirring. The time course of transmittance at 570 nm was monitored by the spectrophotometer.

2.2.5 Simultaneous measurement of the transmittance and redox potential

The redox potential measurements of polymer solutions were performed simultaneously with the transmittance measurement. The redox potential measurements were conducted by utilizing the potentiostat (Hokuto Denko Corp., HA-150G) with Pt electrodes. Pt electrodes as a working and counter electrode, respectively, were placed into an optical cell with a starring bar. Hg/Hg_2SO_4 electrode was utilized as a reference electrode. The agar-gelatin mixture gel saturated KNO_3 solution was adopted in order to maintain electrical connection with the polymer solution. The detail of the experimental setup of simultaneous measurement of the redox potential and transmittance was shown in *ref 40*.

2.2.6 Measurement of self-oscillation for poly(NIPAAm-co-Ru(bpy)$_3$-co-AMPS-co-MAPTAC) solution under the acid and oxidant-free condition.

Polymer solutions were prepared by dissolving the polymer (6.5 wt%) into an aqueous solution containing malonic acid (0.3, 0.5 and 0.7M). The change in optical transmittance for theses polymer solutions were measured under constant temperature and stirring. These measurements were carried out with a spectrophotometer (Shimazu, Model UV-2500)

equipped with a thermostatic controller and magnetic stirrers at 570-nm wavelength, which is the isosbestic point for the reduced and oxidized states of the $Ru(bpy)_3$ moiety.

3. Results and discussion

Figure 2 and 3 showed the waveforms of the transmittance self-oscillation for the AMPS-containing polymer solution in the fixed concentration of the two BZ substrates at several temperatures (12 - 27°C) under acid-free condition. The self-oscillation originates from the different solubility of the AMPS-containing polymer chain in the reduced and oxidized states. In the reduced state, the $Ru(bpy)_3$ moiety in the polymer chain has a significant hydrophobic property. This is because the conformation of the bipyridine ligands surrounding the Ru ion induces the aggregation among the intra- and inter-polymer chains. Therefore, the LCST of the polymer chain in the reduced state is lower than that of the poly(NIPAAm) solution, which is 31°C [41]. On the other hand, in the oxidized state, there is no LCST because the oxidized Ru moiety in the polymer chain has the significantly hydrophilic property. This is because the orientation of the bipyridine ligands surrounding the Ru ion in the oxidized state disturbed the interaction among the $Ru(bpy)_3^{3+}$ moieties in the polymer chain. Therefore, the LCST of the AMPS-containing polymer chain disappear in the oxidized state.

As shown in Figure 2(a)-(c), the aggregation-disaggregation self-oscillation caused damping. That is, the amplitude of the transmittance self-oscillation decreased with time originating from the aggregation of the polymer chains. In the BZ reaction, the time in the reduced state is much longer than that in the oxidized state. As a result, the significant hydrophobic Ru moieties in the polymer chain dominantly behaves for the determination of the size of the polymer aggregation in the self-oscillation. As the aggregation-disaggregation self-oscillation repeated, the size of the polymer aggregation increases due to the strong hydrophobic property of the reduced Ru moiety. The polymer aggregation state in the reduced state is thermodynamically more stable in the polymer solution. Therefore, the polymer aggregation hardly dissociate even in the oxidized state. Furthermore, as shown in Figure 2(a)-(c), the lifetimes of the transmittance self-oscillation are much shorter than that in the low temperature condition (See Figure 2(d)-(f)). This is because the solubility of the polymer chain in the reduced state at the low temperature condition (12-18 °C) is higher than that in the high temperature condition (21-27 °C) due to the thermo-responsive NIPAAm component. Therefore, as shown in Figure 2(d)-(f), the self-oscillating polymer chain do not cause the damping in the low temperature condition (12-18°C). Moreover, the width of the waveform for the AMPS-containing polymer solution increases with the decrease in the temperature due to increase in the rate of the BZ reaction. That is because the rate of the BZ reaction follows the Arrenius equation.

In Figure 3(A), in the high [MA] condition ([MA] = 0.2M), the lifetime of the self-oscillation shows little change even when the temperature increases. However, the lifetime of the self-oscillation is significantly shorter than that in the low [MA] condition ([MA] = 0.1M). In addition, we can see the damping behavior in the low temperature condition (see Figure 3(B)). That is because the self-oscillating behavior is much affected by the initial substrate concentrations of the BZ reaction. Especially, the size of the polymer aggregation is significantly affected by the concentration of malonic acid. That is because the concentration of malonic acid exerts influence on the mole fraction of the reduced Ru moiety in the polymer chain [35, 45]. This tendency is explained by the overall process of the BZ reaction

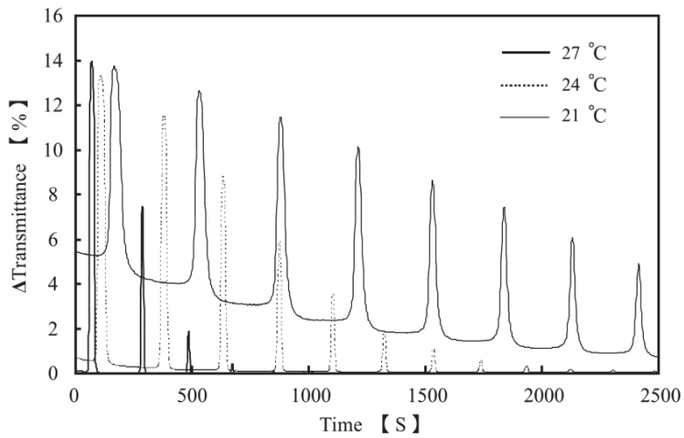
16
14
12
10
8
6
4
2
0
ΔTransmittance 【%】
0
500
1000
1500
2000
2500
Time 【S】
27 ℃
24 ℃
21 ℃

(a)

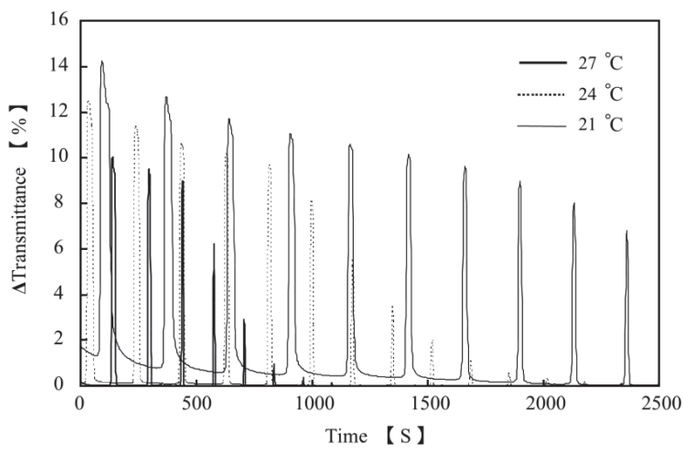
16
14
12
10
8
6
4
2
0
ΔTransmittance 【%】
0
500
1000
1500
2000
2500
Time 【S】
27 ℃
24 ℃
21 ℃

(b)

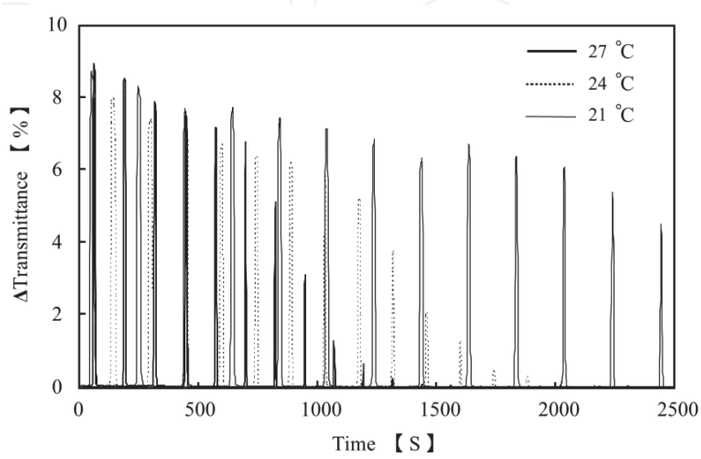
10
8
6
4
2
0
ΔTransmittance 【%】
0
500
1000
1500
2000
2500
Time 【S】
27 ℃
24 ℃
21 ℃

(c)

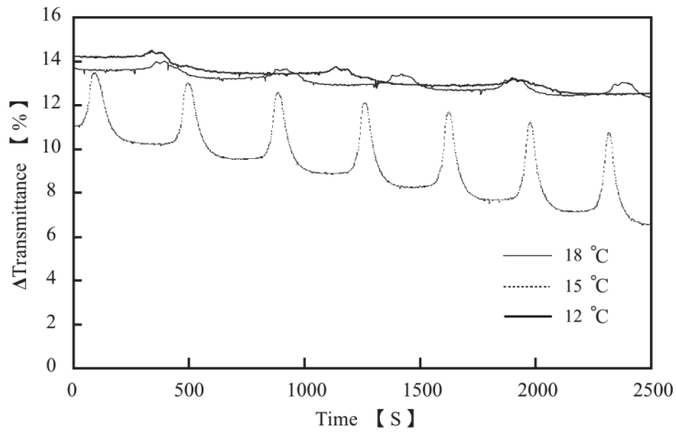

(d)

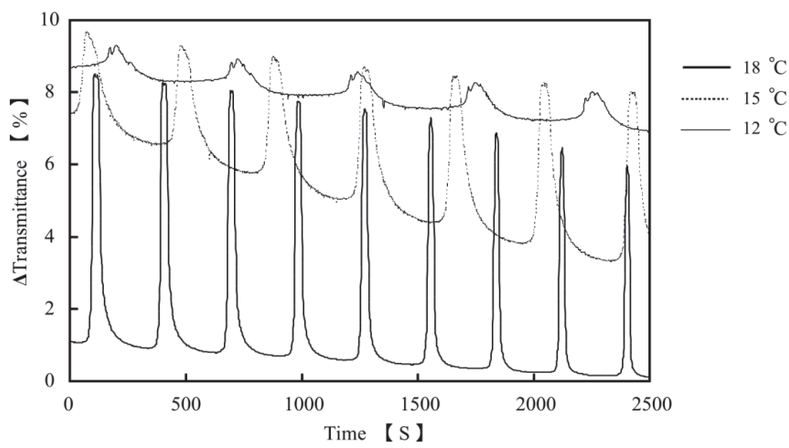

(e)

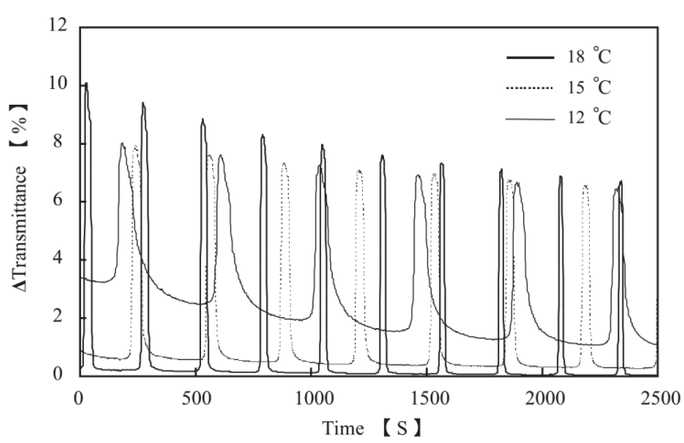

(f)

Fig. 2. Oscillating profiles of the optical transmittance for the 2.5 wt% poly(NIPAAm-*co*-Ru(bpy)$_3$-*co*-AMPS-*co*-AMPS) solutions at 21, 24 and 27 °C (a - c), and 12, 15 and 18 °C (d - e): a, d) [MA] = 0.1 M, [$NaBrO_3$] = 0.4 M, b, e) [MA] = 0.1 M, [$NaBrO_3$] = 0.6 M, c, f) [MA] = 0.1 M, [$NaBrO_3$] = 0.8 M. (Reprinted ref. 35, Copyright Wiley-VCH Verlag GmbH & Co. KGaA. Reproduced with permission.)

based on the Field-koros-Noyes (FKN) mechanism [25-28]. According to the FKN mechanism, the BZ reaction is divided into three main processes: consumption of Br^- ions (process A), autocatalytic formation of $HBrO_2$ (process B), and formation of Br^- ions (process C).

A: $$BrO_3^- + 2Br^- + 3H^+ \rightarrow 3HOBr$$

B: $$BrO_3^- + HBrO_2 + 2Mred + 3H^+ \rightarrow 2HBrO_2 + 2Mox + H_2O$$

C: $$2Mox + MA + BrMA \rightarrow fBr^- + 2Mred + \text{other products}$$

In a process B and C, the reduced $Ru(bpy)_3$ is oxidized (process B), and the oxidized one is reduced (process C) because the Ru moiety works as the catalyst in the BZ reaction. With increasing initial concentration of malonic acid, the mole fraction of the reduced Ru moiety in the polymer chain increases in accordance with the FKN mechanism. As a result, the high mole fraction of the hydrophobic $Ru(bpy)_3^{2+}$ moiety induces the aggregation among the polymer chains in the self-oscillating behavior at the shorter time. Therefore, the lifetime of the self-oscillation decreases with the increase in the concentration of malonic acid. In addition, as shown in Figure 2(a)-(c), with increasing concentration of sodium bromate, the lifetime of the transmittance self-oscillation increases. This is because the high concentration of sodium bromate advances the process C, that is, the mole fraction of the hydrophilic $Ru(bpy)_3^{3+}$ moiety in the polymer chain increases. Therefore, the polymer chains hardly aggregate due to the dissociating force originating from the hydrophilic $Ru(bpy)_3^{3+}$ moiety in the oxidized state. Table 1 summarized the self-oscillating region given by the temperature and the initial concentration of the two BZ substrates. As shown in Table 1, when the [MA] increases, the self-oscillating region becames narrower. In the [MA]=0.3M condition (Table 1(C)), the self-oscillating region is remarkably narrower than that in the [MA]=0.1 and 0.2 M conditions (Table 1(A) and 1(B)). The mole fraction of the significant hydrophobic $Ru(bpy)_3^{2+}$ moiety in the polymer chain increases with increasing concentration of malonic acid. Therefore, in the condition of [MA]=0.3 M, the aggregation disaggregation self-oscillations occur only at the low temperature (12 and 15 °C) in the high $[NaBrO_3]$ condition ($[NaBrO_3]$ = 0.6 and 0.8 M). This is because the solubility of the self-oscillating polymer chain increases with decreasing temperature (effect of the NIPAAm component) and with increasing concentration of sodium bromate (effect of the process B). In all [MA] conditions, no transmittance self-oscillation was observed in the condition of $[NaBrO_3]$ = 0.2 M. This is because the dissociation force originating from the $Ru(bpy)_3^{3+}$ depends on the concentration of sodium bromate.

Figure 5 shows the transmittance self-oscillation of the MAPTAC-containing polymer chain (See Figure 4) at several temperatures under coexistence of the only two BZ substrates (0.1 M malonic acid and 0.3 M sulfuric acid), that is, the self-oscillation occurs under the oxidant-free condition. The BrO_3^- was introduced by the ion exchange method. In order to cause the self-oscillation under the oxidant-free condition, the polymer concentration more than 5.0 wt% is required because the enough amount of the BrO_3^- is necessary for causing the BZ reaction. The LCST of the MAPTAC-containing polymer solution is around 45 °C in the reduced state. On the other hand, there is no LCST in the oxidized state as the same manner of the AMPS-containing polymer solution [34-35]. When the temperature approaches to the LCST of the polymer solution, the amplitude of the self-oscillation gradually decreases. That is because the solubility of the polymer solution decreases in the high temperature conditions due to the thermoresponsive NIPAAm-main chain.

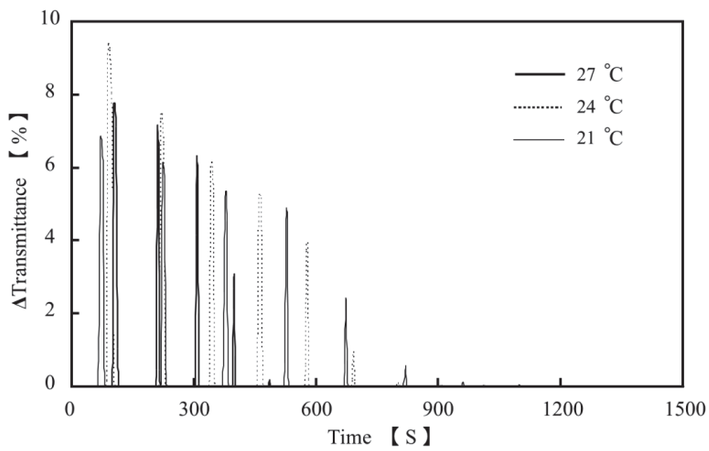

(A)

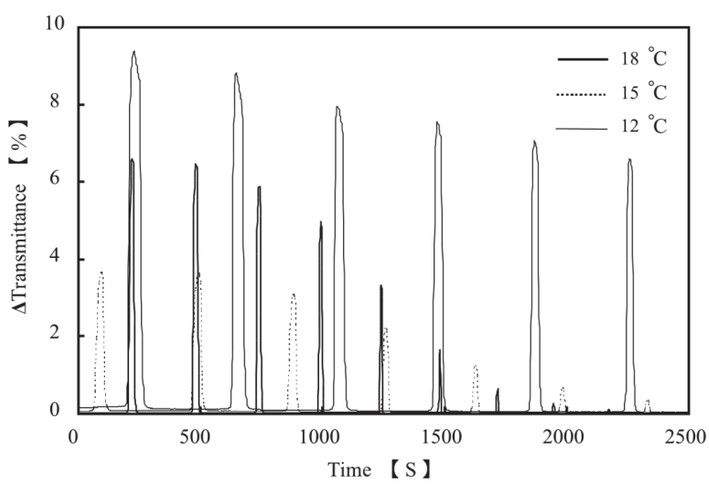

(B)

Fig. 3. Oscillating profiles of the optical transmittance for the 2.5 wt% poly(NIPAAm-*co*-Ru(bpy)$_3$-*co*-AMPS-*co*-AMPS) solutions that contain different initial concentrations of the BZ substrates ([MA] = 0.2 M, [$NaBrO_3$] = 0.6 M) at 21, 24 and 27 °C (A), and 12, 15 and 18 °C (B).) (Reprinted ref. 35, Copyright Wiley-VCH Verlag GmbH & Co. KGaA. Reproduced with permission.)

(A)

Conc. of MA= 0.1M

	Conc. of $NaBrO_3$			
Temperature	0.2 M	0.4 M	0.6 M	0.8 M
12 ℃	×	○	○	○
15 ℃	×	○	○	○
18 ℃	×	○	○	○
21 ℃	×	○	○	○
24 ℃	×	○	○	○
27 ℃	×	○	○	○

(B)

Conc. of MA= 0.2M

	Conc. of $NaBrO_3$			
Temperature	0.2M	0.4M	0.6M	0.8M
12 ℃	×	○	○	○
15 ℃	×	○	○	○
18 ℃	×	×	○	○
21 ℃	×	×	○	○
24 ℃	×	×	○	○
27 ℃	×	×	○	○

(C)

Conc. of MA= 0.3M

	Conc. of $NaBrO_3$			
Temperature	0.2M	0.4M	0.6M	0.8M
12 ℃	×	×	○	○
15 ℃	×	×	○	○
18 ℃	×	×	×	×
21 ℃	×	×	×	×
24 ℃	×	×	×	×
27 ℃	×	×	×	×

Table 1. Phase diagram of the self-oscillating region given by the initial concentration of $NaBrO_3$ and temperature under fixed concentration of MA: (A) [MA] = 0.1 M; (B) [MA] = 0.2 M; (C) [MA] = 0.3 M. The cross means that no self-oscillation occurs. (Reprinted ref. 35, Copyright Wiley-VCH Verlag GmbH & Co. KGaA. Reproduced with permission.)

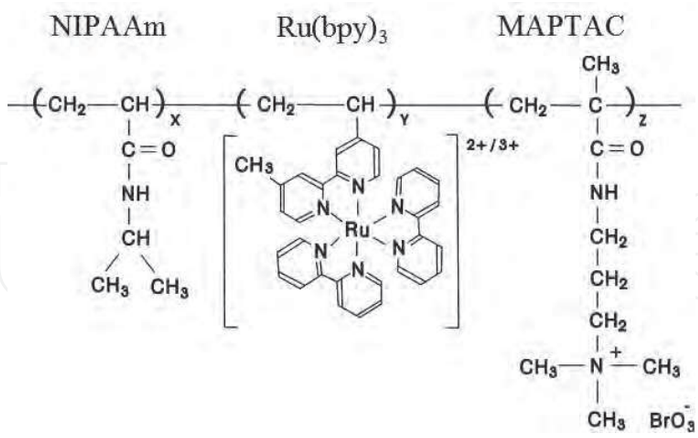

Fig. 4. Chemical structure of poly(NIPAAm-*co*-Ru(bpy)$_3$-*co*-MAPTAC).

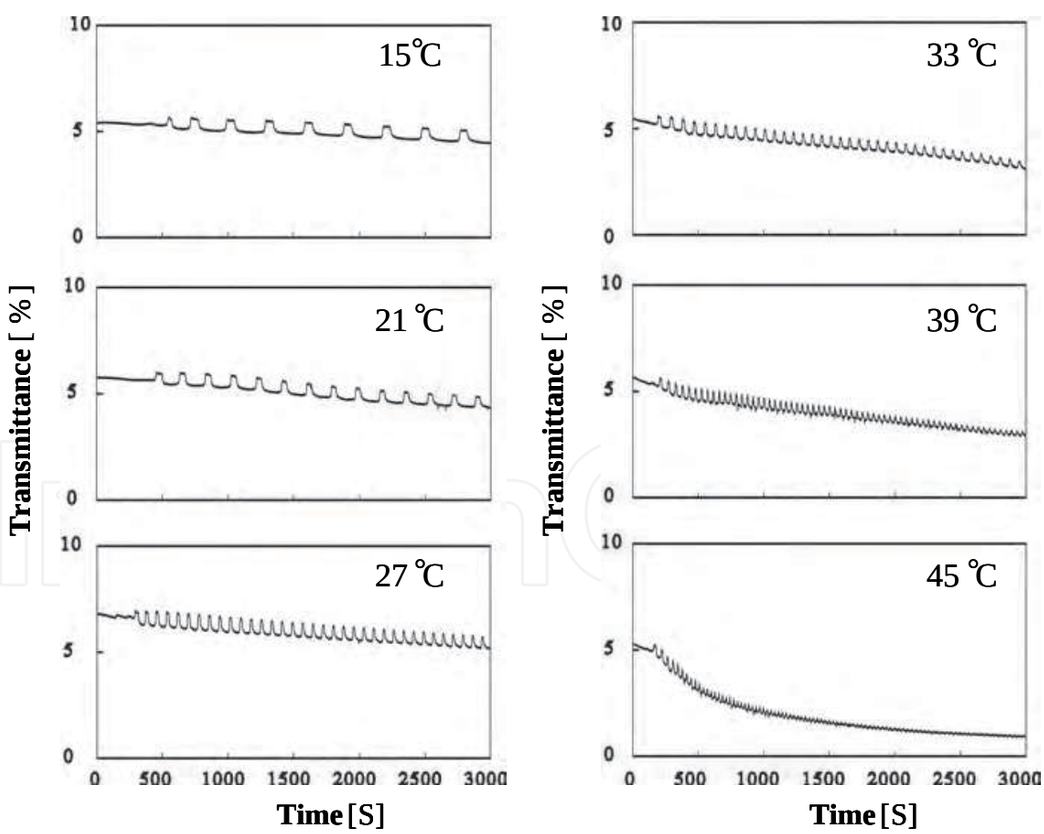

Fig. 5. Oscillating profiles of the optical transmittance for poly-(NIPAAm-*co*-Ru(bpy)$_3$-*co*-MAPTAC) solutions at several constant temperatures (15, 21, 27, 33, 39 and 45 °C). (Reprinted ref. 38, Copyright American Chemical Society. Reproduced with permission.)

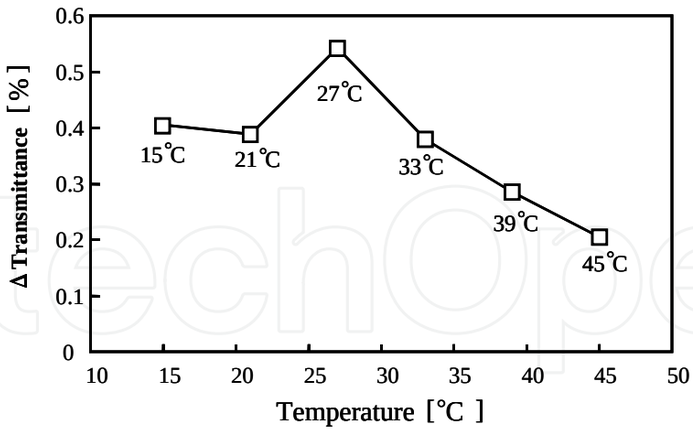

(A)

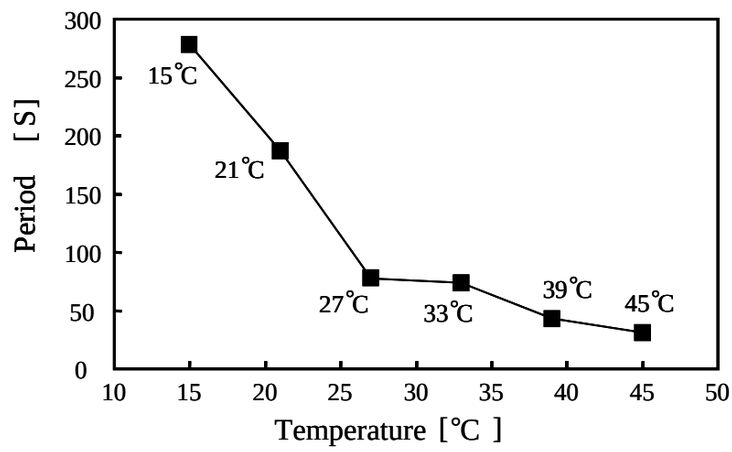

(B)

Fig. 6. Dependence of amplitude (A) and period (B) on temperature for the poly-(NIPAAm-*co*-Ru(bpy)$_3$-*co*-MAPTAC) solutions under the oxidant free-condition. (Reprinted ref. 36, Copyright American Chemical Society. Reproduced with permission.)

Figure 6 shows the amplitude (ΔT%) and the period of the self-oscillation in the several temperature conditions. In all temperature conditions, the amplitude of the self-oscillation is significantly smaller than that of the conventional-type and AMPS-containing self-oscillating polymer solution [33-35]. That is because the driving force of the aggregation-disaggregation self-oscillation is smaller compared to the other self-oscillating polymer chains due to the hydrophilic 65 wt% MAPTAC component. In addition, the small amplitude is considerably affected by the amount of the BrO_3^- in the BZ reaction in accordance with the FKN mechanism as the same manner of the AMPS-containing polymer chain (See Figure 2 and 3). That is because, in this condition, the oxidizing agent was supplied only by the polymer chain. Moreover, as shown in Figure 6(B), the period decreases with increasing temperature. This is a general tendency for the BZ reaction as well known phenomena that the period typically follows the Arrhenius equation.

In order to clarify the different self-oscillating behavior between the poly(NIPAAm-*co*-Ru(bpy)$_3$) and the poly(NIPAAm-*co*-Ru(bpy)$_3$-*co*-MAPTAC), the self-oscillating behavior of the MAPTAC-containing polymer chain (MAPTAC content 0.85 wt%) without BrO_3^- as the counter ion was investigated in the presence of the three BZ substrates other than the Ru catalyst. As shown in Figure 7, LCSTs of the poly(NIPAAm-*co*-Ru(bpy)$_3$) and the poly(NIPAAm-*co*-Ru(bpy)$_3$-*co*-MAPTAC) solutions in the reduced and oxidized states are different due to the hydrophilic 0.85 wt% MAPTAC component. LCST of the conventional-type self-oscillating polymer (poly(NIPAAm-*co*-Ru(bpy)$_3$))solution in the reduced state is 13.0 °C.

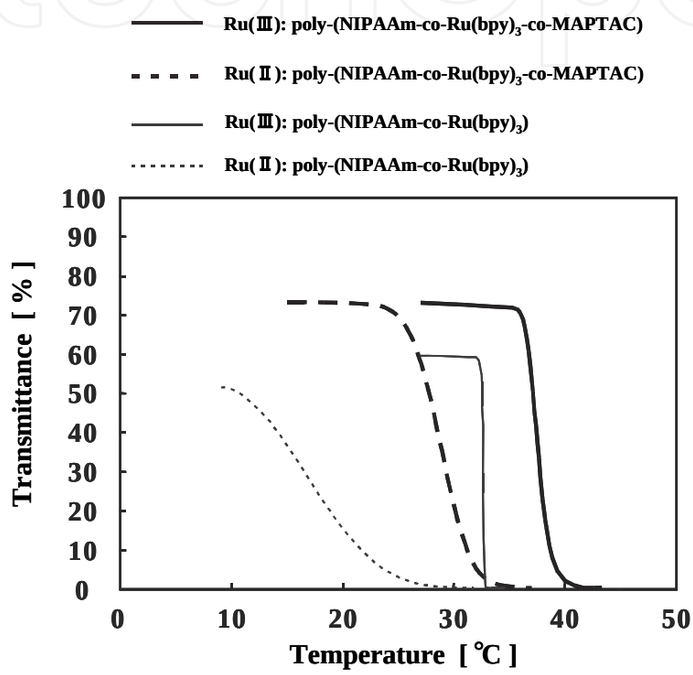

Fig. 7. Temperature dependence of transmittance for poly(NIPAAm-*co*-Ru(bpy)$_3$) and poly(NIPAAm-*co*-Ru(bpy)$_3$-*co*-MAPTAC) solutions under the different conditions of reduced Ru(II) (in Ce(III) solution) and Ru(III) (in Ce(IV) solution) states. (Reprinted ref. 40, Copyright Wiley-VCH Verlag GmbH & Co. KGaA. Reproduced with permission.)

This LCST is considerably lower than that of the poly-NIPAAm solution, which exhibits a LCST around 31°C [41]. This result originates from the hydrophobic effect of the bipyridine ligand surrounding the ruthenium ion in the reduced state. In the reduced state, the Ru moiety in the polymer chain works strongly hydrophobic part. Therefore, the reuced Ru moiety becomes dominant for the determination of the solubility state of the self-oscillating polymer chain. On the contrary, the LCST of the MPATAC-containing polymer solution in the reduced state is 26.5°C. That is because the MAPTAC moiety in the polymer chain obstructs the intra- and inter-molecular interaction originating from the electric repulsive force. Therefore, the LCST of the MAPTAC-containing polymer solution is higher than that of the conventional-type self-oscillating polymer solution. Moreover, in the oxidized state, the LCST of the conventional-type and MAPTAC-containing polymer solution were 32.5°C and 36.5°C, respectively. The oxidized Ru moiety in the polymer chain disturbs the

interaction among the Ru moieties due to the change in the orientation of the bipyridine ligands surrounding the Ru ion. This different solubility of the reduced and oxidized polymer chain is driving force of the transmittance self-oscillation.

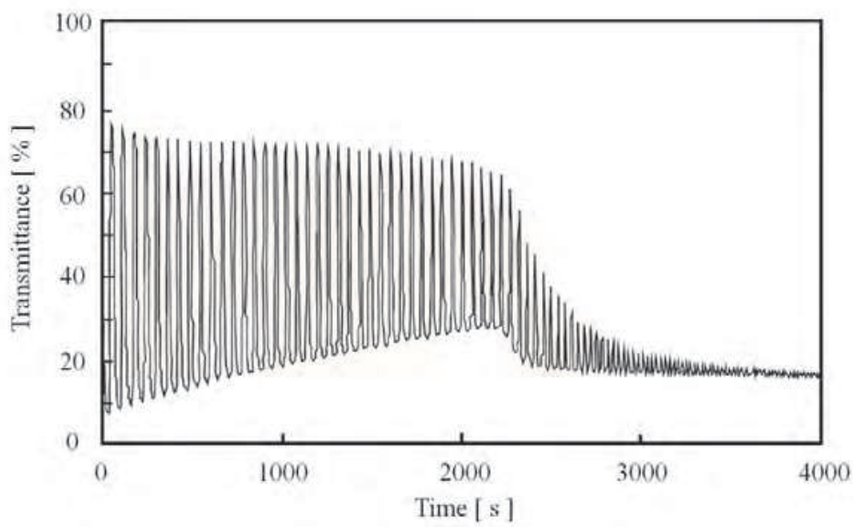

(A)

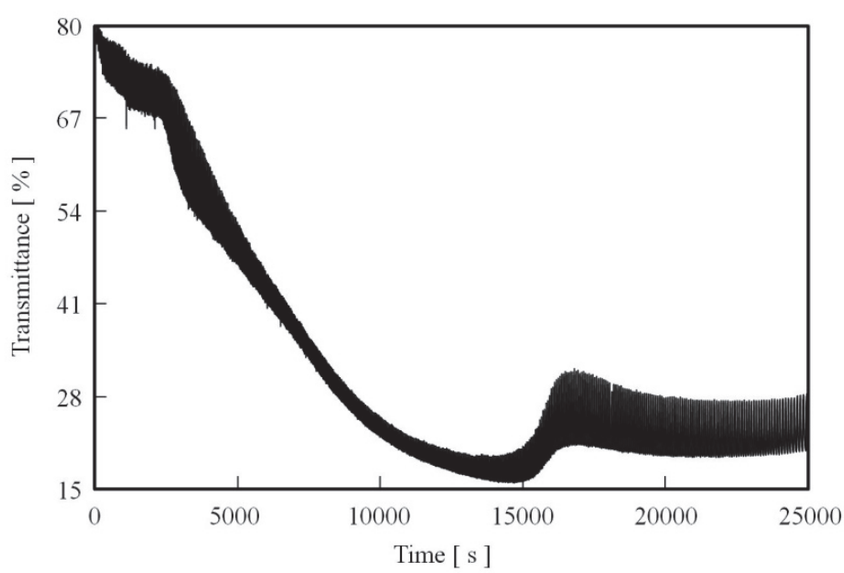

(B)

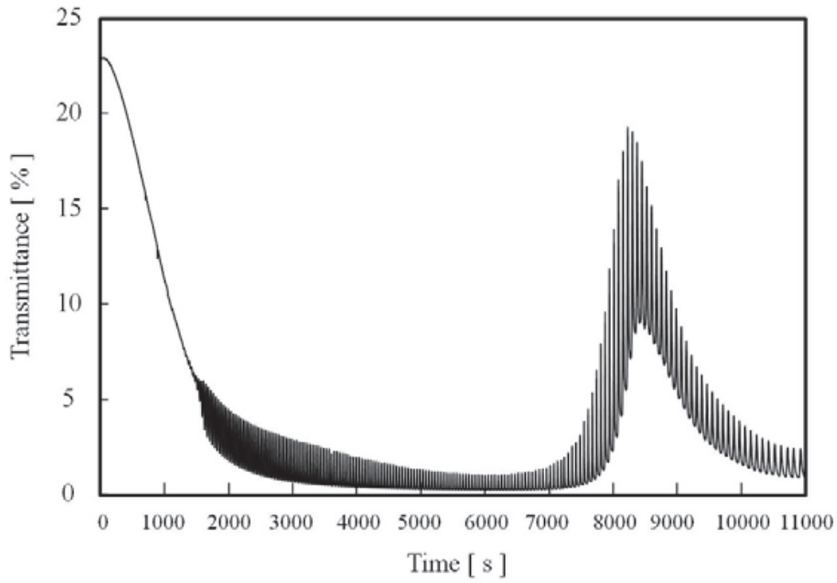

(C)

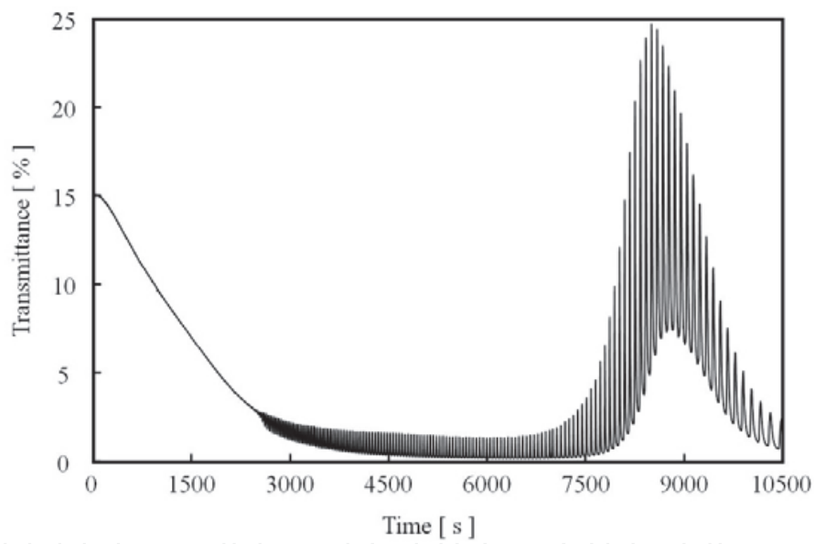

(D)

Fig. 8. Oscillating profiles of transmittance at 20°C for poly(NIPAAm-*co*-Ru(bpy)$_3$): (A) 0.25wt%, and poly(NIPAAm-*co*-Ru(bpy)$_3$-*co*-MAPTAC) solutions at several polymer concentrations: (B) 0.25 wt% , (C) 0.75 wt% and (D) 1.0 wt%. (Reprinted ref. 40, Copyright Wiley-VCH Verlag GmbH & Co. KGaA. Reproduced with permission.)

Figure 8 shows the self-oscillating behaviors of the two types of the polymer solution: One is the conventional-type self-oscillating polymer solution, and the other is MAPTAC-containing one. As shown in Figure 8(A), we can see the damping behavior of the aggregation-disaggregation self-oscillation, that is, the amplitude of the transmittance self-oscillation decreases with time due to the increase in the size of the polymer aggregations. As the aggregation-disaggregaiton self-oscillation repeates, the size of the polymer

aggregation becomes larger. When the size of the polymer aggregation exceeds a threshold, the amplitude of the aggregation-disaggregation self-oscillation drastically decreases. Once the transmittance self-oscillation causes damping, the decreased amplitude never recovers. That is because the polymer aggregation state is thermodynamically more stable in the polymer solution.

Figure 8(B), 8(C) and 8(D) show the self-oscillating behavior of the MAPTAC-containing polymer solution in the condition of different polymer concentrations (0.25, 0.75 and 1.00 wt%). As shown in Figure 8(B), we can see that the decreased amplitude in the early time of the self-oscillation due to the aggregation of the tiny polymer aggregation. However, in the case of the MAPTAC-containing polymer solution, the initially decreased amplitude increased again. This behavior originates from the disaggregation of the large polymer aggregation because of the repulsive force of the cationic MAPTAC domain in the polymer chain. Therefore, this phenomenon is never observed in the case of the conventional-tpye and AMPS-containing polymer solution [33-35].

On the other hand, as shown in Figure 8(C), the transmittance value in the 0.75 wt% was greatly lower than that in the 0.25 wt%. This lower transmittance in the early time attributed to the size of the polymer aggregation. In the early stage of the aggregation-disaggregation self-oscillation, the damping behavior occurred. Subsequently, the initially decreased amplitude increased again. In the condition of the 0.75 wt% for the MAPTAC-containing polymer solution, the degree of the increase in the amplitude was significantly larger than that in the 0.25 wt% due to the dissociation of the larger polymer aggregations. As shown in Figure 8(C), in the next stage of the self-oscillation, the increased amplitude of the transmittance self-oscillation decreased at once because the previously divided tiny polymers aggregated due to the low stable energy of the divided polymer aggregation. Therefore, the re-aggregation phenomenon quickly occurred. In addition, in the 1.00 wt% polymer condition, in the early stage of the transmittance self-oscillation, the self-oscillation did not cause the damping. That is because the initial size of the polymer aggregation was significantly larger than that in the conditions of the low polymer concentration. The degree of the increase in the amplitude in the 1.00 wt% was larger than that in the 0.75 wt% because the size of the polymer aggregation before the disaggregation was larger than that in the 0.75 wt%. However, the increased amplitude in the 1.00 wt% was immediately decreased as the same reason in the 0.75 wt%.

As shown in Figure 8(A) and 8(B), in the same 0.25 wt% polymer condition, the lifetime of the aggregation-disaggregation self-oscillation of the MAPTAC-containing polymer solution is considerably longer than that of the conventional-type self-oscillating polymer solution. In the case of the MAPTAC-containing polymer solution, the cationic MAPTAC component inhibits the increase in the size of the polymer aggregation due to the repulsive force among the intra- and inter-polymer chains. Moreover, as shown in Figure 8(B), 8(C) and 8(D), the polymer concentration considerably affected the lifetime of the self-oscillation.

In addition, we challenged the analysis of the detail mechanisms of the damping and re-aggregation phenomenon. However, the detail analysis of the aggregation-disaggregation self-oscillation is significantly difficult because the self-oscillation occurred on the nonlinear and non-equilibrium situations. The most conventional analytical techniques regarding the analysis of the polymer solution such as a dynamic light scattering, etc. provide only the data of the polymer solution on the equilibrium state. Therefore, it is difficult to obtain the sufficient information of the dynamics of the aggregation-disaggregation self-oscillation.

Therefore, in this investigation, the simultaneous measurement of the tranmittance and redox potential was conducted because the redox potential indicates the time-dependent data of the mole fraction of the reduced and oxidized $Ru(bpy)_3$ moiety in the polymer solution in accordance with the Nernst equation. By utilizing the time-dependent data of the redox potential, the dynamics of the self-oscillating behavior was analyzed because the solubility of the polymer chain is determined by the redox state of the Ru moiety.

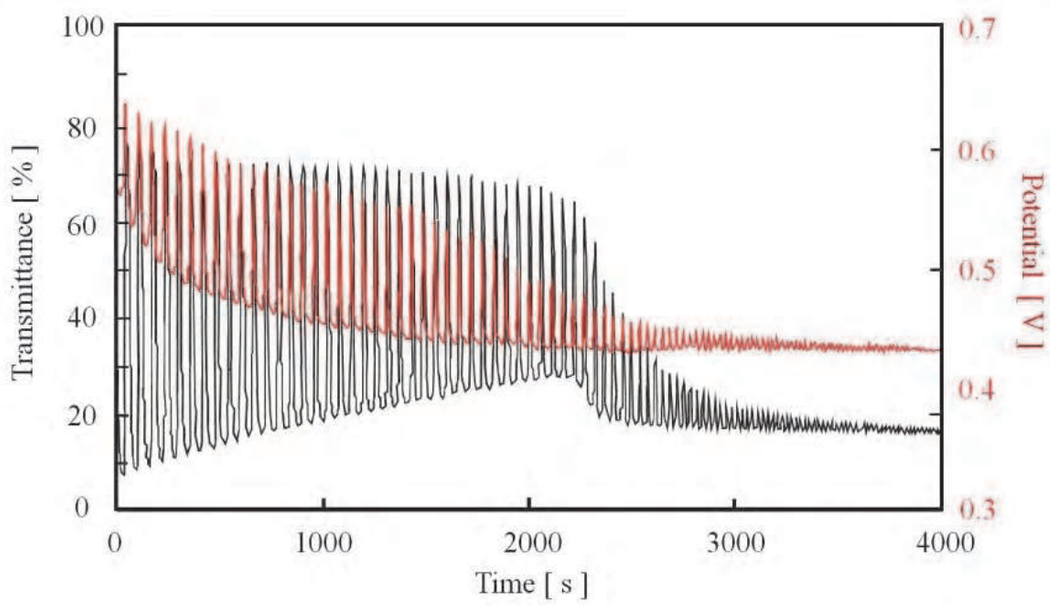

(A)

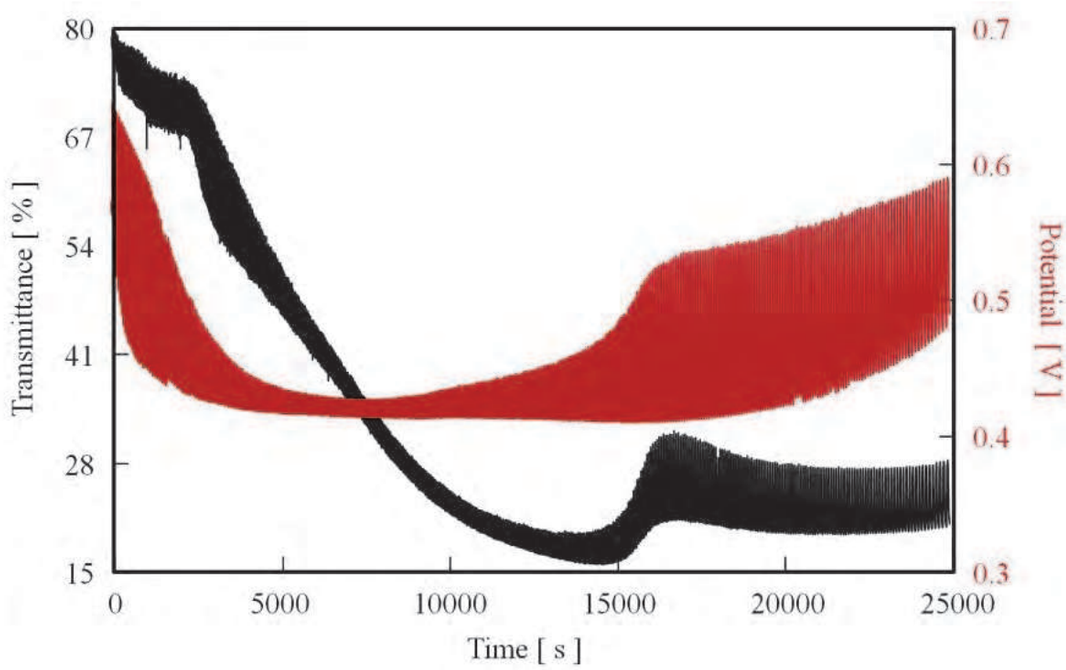

(B)

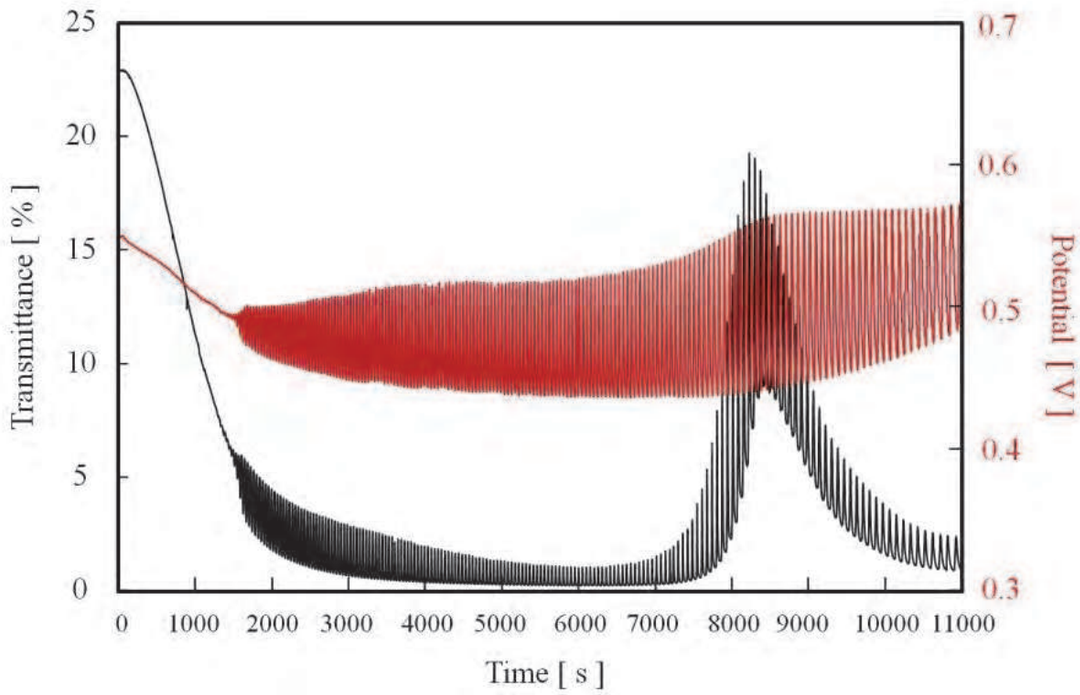

(C)

Fig. 9. Oscillating profiles of the redox potential for poly(NIPAAm-*co*-Ru(bpy)$_3$) solution: (A) 0.25wt% at 20°C, and poly(NIPAAm-*co*-Ru(bpy)$_3$-*co*-MAPTAC) solutions at several polymer concentration: (B) 0.25wt% , (C) 0.75wt% at 20°C. (Reprinted ref. 40, Copyright Wiley-VCH Verlag GmbH & Co. KGaA. Reproduced with permission.)

Figure 9 shows the results of the simultaneous measurement of the redox potential and transmittance. As shown in Figure 9(A), the amplitude of the redox self-oscillation decreases with time. This behavior indicated that the reactivity of the Ru(bpy)$_3$ moiety in the polymer solution decreases because of the increase in the polymer aggregation. That is because the Ru(bpy)$_3$ moieties into the polymer aggregation are obstructed the collision of the other BZ substrates by the polymer chain. With the increase in the size of the polymer aggregation, the number of the non-reacted Ru(bpy)$_3$ moiety inside the polymer aggregation increases as well. Finally, the transmittance and redox self-oscillations completely stop at the same time due to the decrease in the reactivity of the Ru(bpy)$_3$ moiety in the polymer cahin.

On the other hand, as shown in Figure 9(B), the amplitude of the redox self-oscillation decreases with time due to the increase in the polymer aggregation. Subsequently, the amplitude of the redox self-oscillation increases again after 7500 seconds due to the repulsive force of the MAPTAC moieties. In general, when assuming that the two-types of polymer chains (one is charged polymer, and the other is non-charged polymer chain) are the same length, the hydrodynamic radius of the charged polymer chain is larger than that of the non-charged polymer chain. As the number of the charged component in the polymer chain increases, this tendency becomes lager. Moreover, as the hydrodynamic radius of the polymer chain increases, the density of the polymer chain that constitutes the aggregation decreases as well. Therefore, the density of the MAPTAC-containing polymer chain inside the aggregation is lower than that of the conventional-type self-oscillating polymer chain. In the high density of the polymer chain (See Figure 9(A)), the polymer chains obstruct the

collision between the $Ru(bpy)_3$ moieties and the other BZ substrate, That is, the reaction field of the Ru moiety inside the polymer aggregation with the low polymer density (MAPTAC-containing polymer) is larger than that in the polymer aggregation compared with the high polymer density (conventional-type poly(NIPAAm-co-Ru(bpy)3)). As shown in Figure 9(B), when the amplitude of the redox self-oscillation increased, the reaction rate of the $Ru(bpy)_3$ moiety per one cycle of the BZ reaction increases as well. As a result, the density of the polymer chain in the polymer aggregation decreases due to the repulsive force of the reactive $Ru(bpy)_3$ moiety. In this situation, the reaction rate of the $Ru(bpy)_3$ moiety inside the aggregation received the positive feedback from the change in the density of the polymer chain. As the reactivity of the $Ru(bpy)_3$ moiety inside the polymer aggregation exceeded a threshold, the decreased amplitude of the transmittance self-oscillation increases again. As shown in Figure 9(C), the amplitude of the redox self-oscillation increased at the starting point because the size of the polymer aggregation in 0.75 wt% is larger than that in 0.25 wt%. In this condition, the strength of the positive feedback of the reactivity of the $Ru(bpy)_3$ moiety in 0.75 wt% is larger than that in the 0.25 wt% due to the larger number of the Ru moiety per a polymer aggregation. As a consequence, the amplitude of the redox self-oscillation increased continuously from the start point of the self-oscillation, and then the amplitude of the transmittance self-oscillation increases again.

As the final step for causing the self-oscillation under the acid and oxidant free condition, poly(NIPAAm-*co*-$Ru(bpy)_3$-*co*-AMPS-*co*-MAPTAC) was synthesized (See Figure 10).

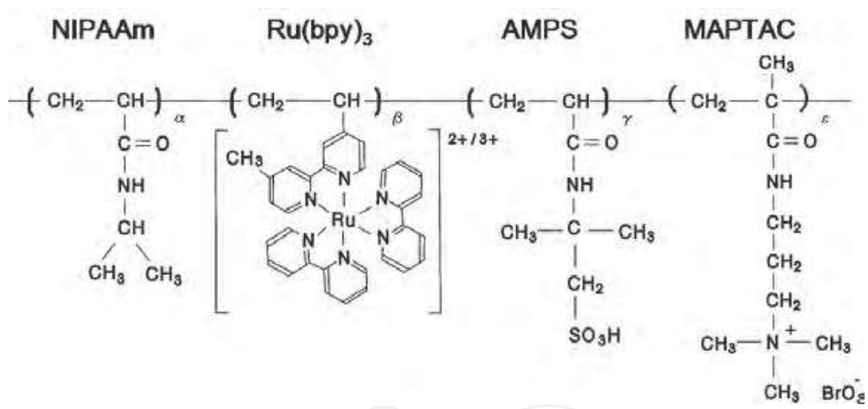

Fig. 10. Chemical structure of poly(NIPAAm-*co*-$Ru(bpy)_3$-*co*-AMPS-*co*-MAPTAC).

This polymer chain has the pH control and oxidant supply sites coexist in the polymer chain at the same time. Figure 11 shows the aggregation-disaggregation self-oscillation of the novel polymer solutions at the constant temperature under coexistence with only one bio-related BZ substrate (malonic acid). The novel polymer chain supplied H^+, BrO_3^- and Br^- ions as counter ions from the AMPS, MAPTAC and $Ru(bpy)_3$ sites, respectively. In order to cause the self-oscillation in the only malonic acid adding condition, sufficient amounts of H^+, BrO_3^- and Br^- ion are needed. Therefore, the aggregation-disaggregation self-oscillation in the polymer concentration is not observed below 6.5 wt%. Moreover, as shown in Figure 11, the aggregation-disaggregation self-oscillation caused damping with time due to the interaction among the intra- and inter-polymer chain originating from the interaction between the anionic AMPS and cationic MAPTAC moieties. Figure 12 shows the oscillation periods plotted as a function of the concentration of malonic acid. As shown in Figure 12, the period of the aggregation-disaggregation self-oscillation of the novel polymer chain is

proportional to the concentration of malonic acid. By utilizing the proportional relationship between the period and the concentration of malonic acid, the existing malonic acid concentration can be calculated by measuring the period of the novel self-oscillating polymer solution. Therefore, the novel polymer solution can be applied as a novel sensor, which can measure the concentration of an organic acid.

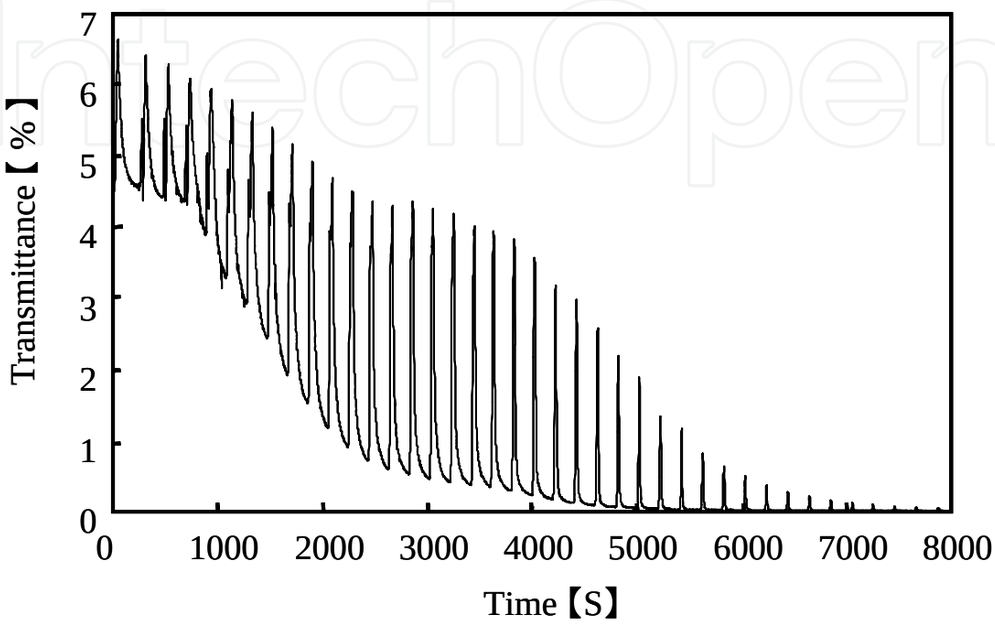

(A)

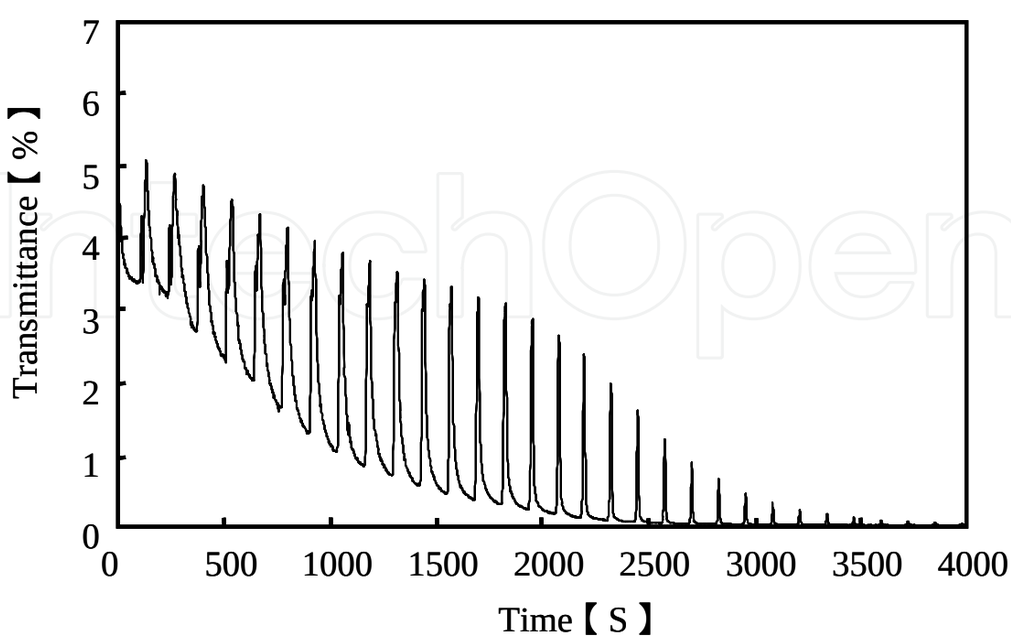

(B)

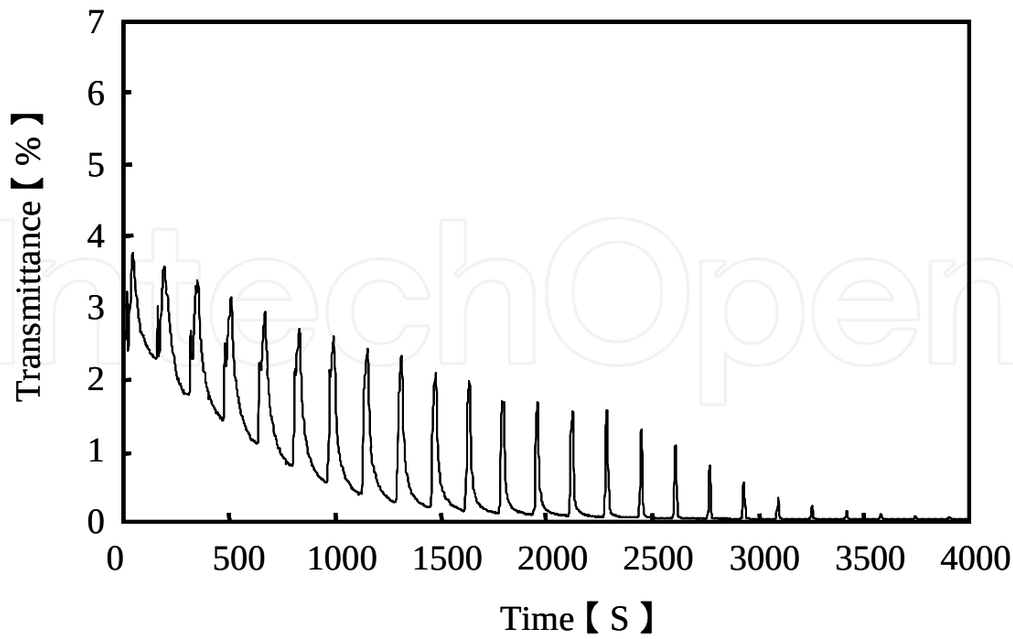

(C)

Fig. 11. Oscillating profiles of the optical transmittance for the poly(NIPAAm-*co*-Ru(bpy)$_3$-*co*-AMPS-*co*-MAPTAC) solutions at 12 °C for several concentrations of malonic acid: (A) [MA] = 0.3 M, (B) [MA] = 0.5 M, (C) [MA] = 0.7 M. (Reprinted ref. 39, Copyright American Chemical Society. Reproduced with permission.)

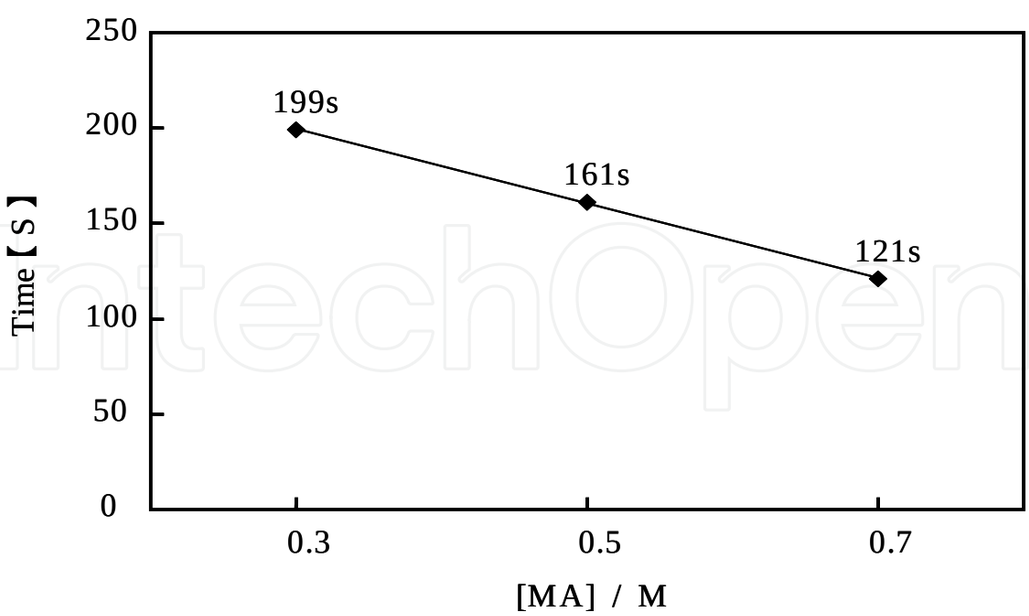

Fig. 12. Dependence of the period on the concentration of malonic acid for the poly(NIPAAm-*co*-Ru(bpy)$_3$-*co*-AMPS-*co*-MAPTAC) solutions at 12 °C. (Reprinted ref. 39, Copyright American Chemical Society. Reproduced with permission.)

4. Conclusion

In this Chapter, the self-oscillating behaviors of many types of self-oscillating polymer chains were reported. The AMPS-containing polymer chain is significantly affected by the temperature and the initial concentration of the two BZ substrates under the acid-free condition. In the case of the MPATAC-containing polymer chain, the damping behavior was observed at only near the LCST under the oxidant-free condition. In addition, in the case of the MAPTAC-containing polymer chain without the BrO_3^- as the counter ion, the phenomenon that the initially decreased amplitude increased again was observed. This phenomenon originates from the autonomous dissociation of the polymer aggregation in the self-oscillating behavior. Moreover, in the last part of this Chapter, the transmittance self-oscillating behavior in a only malonic acid existing condition was introduced. This self-oscillation utilized the novel self-oscillating polymer chain with the pH control and oxidant supply sites at the same time. As for the novel quarternary polymer chain, the effect of the malonic acid concentration on the self-oscillating behavior was studied. As a result, the relationship between the period and the concentration of the malonic acid was shown to be a good straight-line relation.

5. Acknowledgment

The author gratefully thanks prof. Ryo Yoshida (Univ. Tokyo) and prof. Shuji Hashimoto (Waseda Univ.) on these researches.

6. References

[1] Tanaka, T. (1981). Gels, *Scientific American.*,244, pp.110-116, ISSN 0036-8733

[2] Hirokawa, Y.; Tanaka, T. (1984). Volume phase transition in a non ionic gel, *Journal of chemical Physics*, 81, pp.6379-6380, ISSN *0021-9606*

[3] Ilmain, F.; Tanaka, T., Kokufuta, E. (1991). Volume transition in a gel by hydrogen bonding, *Nature,* 349, pp.400-401, ISSN 0028-0836

[4] Tanaka, T. (1978). Collapse of gels and critical endpoint, *Physical Review Letters*, 40, pp.820-823, ISSN 0031-9007

[5] Suzuki, A.; Tanaka, T. (1990). Phase transition in a polymer gels induced by visible-light, *Nature,* 346, pp. 345-347, ISSN 0028-0836

[6] Fukushima, T.; Asaka, K.; Kosaka, A.; Aida, T. (2005). Fully plastic actuator through layer-by-layer casting with ionic-liquid-based bucky gel. Angewandte Chemie International Edition, 44, pp.2410-2413, ISSN 1433-7851

[7] Oguro, K.; Kawami, Y.; Takenaka, H. (1992). An actuator element of polyelectrotyte gel membrane-electrode composite, *Bulletin of the Government Industrial Research Institute, Osaka*, 43, pp. 21–24 ISSN ??

[8] Peppas, N. A.; Hilt, J. Z.; Khademhosseini, A.; Langer, R. (2006). Hydrogels in Biology and Medicine: From Molecular Principles to Bionanotechnology, *Advanced Materials*, 18, pp.1345-1360 ISSN 1521-4095

[9] Steinberg, I, Z.; Oplatka, A.; Kachalsky, A. (1996). Mechanochemnical engines, *Nature,* 210, pp. 568–571, ISSN 0028-0836

[10] Beebe, D. J.; Moore, J. S.; Bauer, J. M.;Yu, Q.;Liu, R. H.;Devadoss, C.; Jo, B. H. (2000). Functional hydrogel structures for autonomous flow control inside microfluidic channels, *Nature,* 404, pp. 588-590, ISSN 0028-0836

[11] Kim, J.; Nayak, S.; Lyon, L. A. (2005). Bioresponsive hydrogel microlenses, *Journal of the American Chemical Society*, 127, pp. 9588–9592 ISSN 0002-7863

[12] Hoffman, J.; Plotner, M.; Kuckling, D.; Fischer, W. (1999). Photopatterning of thermally sensitive hydrogels useful for microactuators, *Sensors and Actuators B: Chemical,* 77, pp. 139–144, ISSN 0925-4005

[13] Moorthy, J.; Beebe, D. J. (2003). Organic and biomimetic designs for microfluidic systems – new strategies offer a flexible approach to designing microscale devices, *Analytical Chemistry*, 2003, 75, pp. 292A–301A ISSN 0003-2700

[14] Hoffman, A. S. (2002) Hydrogels for biomedical applications, *Advanced Drug Delivery Reviews*, 43, pp. 3-12, ISSN 0169-409X

[15] Tanaka, T.; Nishio, I.; Sun, S. T.; Ueno-nishio, S. (1982). Collapse of Gels in an Electric Field, *Science,* 218, pp. 467-469, ISSN 1095-9203

[16] Dong, L.; Jiang, H. (2007). Autonomous microfluidics with stimuli-responsive hydrogels, *Soft Matter*, 3, pp. 1223-1230, ISSN 1744-683X

[17] Kwon, I. C.; Bae, Y. H.; Kim, S. W. (1991). Electrically credible polymer gel for controlled release of drugs. *Nature*, 354, pp. 291-293 ISSN 0028-0836

[18] Harada, A. ; Kataoka, K. (1999). Chain length recognition: core-shell supramolecular assembly from oppositely charged block copolymers. *Science*, 283, pp. 65-67 ISSN 1095-9203

[19] Miyata, T., Asami, N. ; Uragami, T. (1999) A reversible antigenresponsive hydrogel, *Nature*, 399, pp. 766–796, ISSN 0028-0836

[20] Kataoka, K.; Miyazaki, H.; Bunya, M.; Okano, T.; Sakurai, Y. (1998). Totally synthetic polymer gels responding to external glucose concentration: their preparation and application to on-off regulation of insulin release, *Journal of the American Chemical Society*, 120, pp. 12694-12695, ISSN 0002-7863

[21] Yoshida, R.; Uchida, K.; Kaneko, Y.; Sakai, K.; Kikuchi, A.; Sakurai, Y.; Okano, T. (1995). Comb-type grafted hydrogels with rapid de-swelling response to temperature changes, *Nature*, 374, pp. 240-242, ISSN 0028-0836

[22] Zaikin, A.N.; Zhabotinsky, A.M. (1970). Concentration Wave propagation in two-dimensional liquid-phase self-oscillating system, *Nature,* 225, pp. 535–537, ISSN 0028-0836

[23] Reusser, E.J.; Field, R.J. (1979). The transition from phase waves to trigger waves in a model of the Zhabotinskii reaction, *Journal of the American Chemical Society*, 101, pp. 1063–1071, ISSN 0002-7863

[24] Nicolis, G.; Prigogine, I. (1997). Self Orgainization in Nonequilibrium Systems; *Wiley: New York, NY, USA.*

[25] Field, R.J.; Burger, M. (1985). Oscillations and Traveling Waves in Chemical Systems; *John Wiley & Sons: New York, NY, USA.*

[26] Field, R.J.; Noyes, R. M. (1974). Oscillations in chemical systems. IV. Limit cycle behavior in a model of a real chemical reaction, *Journal of Chemical Physics*, 60, pp. 1877–1884, ISSN 0021-9606

[27] Gyorgyi, L.; Turanyi, T.; Field, R J. (1990). Mechanistic details of the oscillatory Belousov-Zhabotinskii reaction, *Journal of Chemical Physics*, 94, pp. 7162–7170, ISSN 0021-9606

[28] Turanyi, T.; Gyorgyi, L.; Field, R. J. (1993), Analysis and simplification of the GTF model of the Belousov-Zhabotinsky reaction, *Journal of Chemical Physics*, 97, pp. 1931–1941, ISSN 0021-9606

[29] Scott, S. K. (1991), Chemical Chaos, *1st ed.; Oxford University Press: Oxford, UK*.

[30] Mori, H. ; Kuramoto, Y. (1997). Dissipative Structures and Chaos, *Springer-Verlag, Berlin*.

[31] Ishiwatari, T.; Kawaguchi, M.; Mitsuishi, M. (1984). Oscillatry reactions in polymer systems, *Journal of Polymer Science Part A: Polymer Chemistry*, 22, pp. 2699-2704 ISSN 0887-624X

[32] Yoshida, R.; Takahashi, T.; Yamaguchi, T.; Ichijo, H. (1996). Self-oscillating gel, *Journal of the American Chemical Society*, 118, pp. 5134-5135, ISSN 0002-7863

[33] Yoshida, R.; Sakai, T.; Ito, S.; Yamaguchi, T. (2002). Self-oscillation of polymer chains with rhythmical soluble-insoluble changes, *Journal of the American Chemical Society*, 124, pp. 8095-8098, ISSN 0002-7863

[34] Hara, Y.; Yoshida, R. Self-oscillation of polymer chains induced by the Belousov-Zhabotinsky reaction under acid-free conditions. *Journal of Physical Chemistry B* 2005, 109, pp. 9451–9454, ISSN 1089-5647

[35] Hara, Y.; Yoshida, R. (2009). Damping behavior of aggregation-disaggregation self-oscillation for a polymer chain, *Macromolecular Rapid Communications*, 30, pp. 1656–1662, ISSN 1521-3927

[36] Hara, Y.; Yoshida, R. (2005). Control of oscillating behavior for the self-oscillating polymer with pH-control site, *Langmuir*, 21, pp. 9773–9776, ISSN 0743-7463

[37] Hara, Y.; Yoshida, R. (2008). A viscosity self-oscillation of polymer solution induced by the BZ reaction under acid-free condition, *Journal of Chemical Physics*, 128, 224904, ISSN 0021-9606

[38] Hara, Y.; Sakai, T.; Maeda, S.; Hashimoto, S.; Yoshida, R. (2005).b Self-oscillating soluble-insoluble changes of polymer chain including an oxidizing agent induced by the Belousov-Zhabotinsky reaction, *Journal of Physical Chemistry B,* 109, pp. 23316–23319, ISSN 1089-5647

[39] Hara, Y.; Yoshida, R. (2008). Self-oscillating polymer fueled by organic acid. *Journal of Physical Chemistry B,* 112, pp. 8427–8429, ISSN 1089-5647

[40] Hara, Y.; Yoshida, R. (2009). Influence of a positively charged moiety on aggregation-disaggregation self-oscillation induced by the BZ reaction, *Macromolecular Chemistry and Physics*, 210, pp. 2160–2166, ISSN 1022-1352

[41] Heskins, M.; Guillet, J. E. (1968). Solution properties of poly(N-isopropylacrylamide) *Journal of Macromolecular Science*, A2, pp. 1441-1455, ISSN 1060-1325

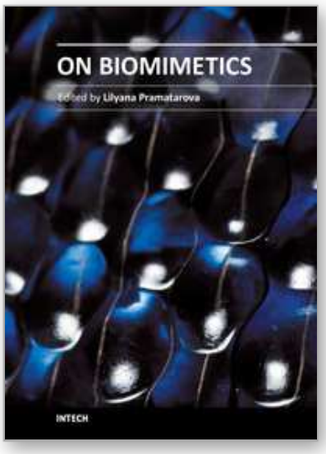

On Biomimetics

Edited by Dr. Lilyana Pramatarova

ISBN 978-953-307-271-5
Hard cover, 642 pages
Publisher InTech
Published online 29, August, 2011
Published in print edition August, 2011

Bio-mimicry is fundamental idea â€˜How to mimic the Natureâ€™ by various methodologies as well as new ideas or suggestions on the creation of novel materials and functions. This book comprises seven sections on various perspectives of bio-mimicry in our life; Section 1 gives an overview of modeling of biomimetic materials; Section 2 presents a processing and design of biomaterials; Section 3 presents various aspects of design and application of biomimetic polymers and composites are discussed; Section 4 presents a general characterization of biomaterials; Section 5 proposes new examples for biomimetic systems; Section 6 summarizes chapters, concerning cells behavior through mimicry; Section 7 presents various applications of biomimetic materials are presented. Aimed at physicists, chemists and biologists interested in biomineralization, biochemistry, kinetics, solution chemistry. This book is also relevant to engineers and doctors interested in research and construction of biomimetic systems.

How to reference

In order to correctly reference this scholarly work, feel free to copy and paste the following:

Yusuke Hara (2011). Molecular Design of Novel Self-Oscillating Polymer Chains Fuelled by Organic Acid Under Constant Condition, On Biomimetics, Dr. Lilyana Pramatarova (Ed.), ISBN: 978-953-307-271-5, InTech, Available from: http://www.intechopen.com/books/on-biomimetics/molecular-design-of-novel-self-oscillating-polymer-chains-fuelled-by-organic-acid-under-constant-con

INTECH
open science | open minds

InTech Europe
University Campus STeP Ri
Slavka Krautzeka 83/A
51000 Rijeka, Croatia
Phone: +385 (51) 770 447
Fax: +385 (51) 686 166
www.intechopen.com

InTech China
Unit 405, Office Block, Hotel Equatorial Shanghai
No.65, Yan An Road (West), Shanghai, 200040, China
中国上海市延安西路65号上海国际贵都大饭店办公楼405单元
Phone: +86-21-62489820
Fax: +86-21-62489821